# Growth of Nanostructured Diamond, Diamond-Like Carbon, and Carbon Nanotubes in a Low Pressure Inductively Coupled Plasma

Katsuyuki Okada

National Institute for Materials Science, 1-1 Namiki, Tsukuba, Ibaraki 305-0044, Japan,
okada.katsuyuki@nims.go.jp

## ABSTRACT

A 13.56 MHz low pressure inductively coupled $CH_4/CO/H_2$ plasma has been applied to prepare nanocrystalline diamond particles of 200-700 nm diameter. The minimum diameter of the particles was found to be 5 nm. Two-dimensional platelet-like graphite and carbon nanotubes also were deposited with different conditions. The characterizations were performed with transmission electron microscopy (TEM) and electron energy loss spectroscopy (EELS). The TEM observations have revealed that the two-dimensional platelet-like deposits consist of disordered microcrystalline graphite, whereas the particles are composed of only diamond nanocrystallites. The high-resolution TEM images clearly show that each particle is composed of small particles of about several ten nm in diameter. The mapping of $sp^2$ bonding by the $\pi^*$ image reveals that $sp^2$-bonded carbons are localized in the grain boundaries of 20-50 nm sub-grains of nanocrystalline diamond particles at approximately 1 nm width.

***Keywords***: nanocrystalline diamond, nanostructured carbon, inductively coupled plasma, electron energy loss spectroscopy, $sp^2/sp^3$ bonding,

## 1 INTRODUCTION

Nanocrystalline diamond and nanostructured carbon films have attracted considerable attention because they have a low coefficient of friction and a low electron emission threshold voltage [1]. The small grain size (approximately 5-100 nm) gives films valuable tribological and field-emission properties comparable to those of conventional polycrystalline diamond films. Furthermore, applications for micro-electro-mechanical systems (MEMS) devices, metal-semiconductor field effect transistors (MESFETs), electrochemical electrodes, and biochemical devices have been proposed that take advantage of these excellent properties [2-4].

A 13.56 MHz low pressure inductively coupled $CH_4/CO/H_2$ plasma has been applied to prepare nanocrystalline diamond particles of 200-700 nm diameter. The minimum diameter of the particles was found to be 5 nm. Two-dimensional platelet-like graphite and carbon nanotubes also were deposited with different conditions. The characterizations were performed with transmission electron microscopy (TEM) and electron energy loss spectroscopy (EELS).

## 2 EXPERIMENT

The schematic view of the low pressure ICP-CVD system is illustrated in Figure 1. The detailed description and deposition procedures were reported previously [5]. To be brief, a low pressure ICP was generated in a growth chamber by applying 13.56 MHz rf powers of 1 kW to a three-turn helical antenna. The flow rates of $CH_4$ and $H_2$ were kept at 4.5 and 75 sccm, respectively, whereas the flow rate of CO ([CO]) was varied between 0, 1.0, and 10 sccm, respectively. The total gas pressure was accordingly varied from 45 to 50 mTorr. Silicon (100) wafers (10 mm in diameter) were used as a substrate. The substrate temperature was kept at 900 ℃. The deposition duration was 2 h.

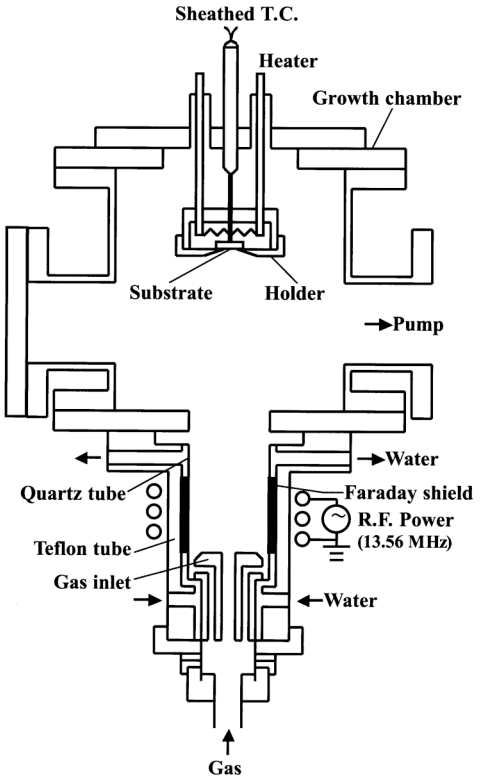


Fig. 1. Schematic description of the low pressure inductively coupled rf plasma CVD system.


NSTI-Nanotech 2008, www.nsti.org, ISBN 978-1-4200-8503-7 Vol. 1

EELS measurements [6] were carried out by using a post-column energy filter (GATAN, GIF2002) equipped with a transmission electron microscope (TEM; Hitachi HF-3000) at 297 keV.

## 3 RESULTS & DISCUSSION

### 3.1 Morphology

Figure 2 shows SEM photographs of the resultant deposits on a Si(100) substrate. Figs. 2(a), 2(b), and 2(c) correspond to [CO]=0, 1.0, and 10 sccm, which are referred to as samples A, B, and C, respectively. The morphology of sample A was platelet-like, as shown in Fig. 2(a), and no crystal facets were clearly seen. When CO was added to the $CH_4/H_2$ plasma, particles of 200-300 nm diameter as well as platelet-like deposits appeared, as shown in Fig. 2(b). With the increase in [CO], only particles were deposited on the Si substrate, as shown in Fig. 2(c). The diameters of the particles were 200-700 nm. Detailed observation reveals that the particles consist of small particles of about 20-50 nm diameter, and that the particle size remains are almost the same regardless of increasing [CO]. It is therefore speculated that increasing [CO] results in a large supersaturation degree of carbon; thus, the number of encounters between particles is increased.

The previous TEM observations have revealed [5] that the two-dimensional platelet-like deposits consist of disordered microcrystalline graphite, whereas the particles are composed of only diamond nanocrystallites. The high-resolution TEM images clearly show that each particle is composed of small particles of about several ten nm in diameter. The X-ray diffraction pattern for the sample C exhibits the diffraction peaks of diamond (111) and (220) planes [7]. The crystallite size was estimated to be approximately 20 nm from the full width at half maximum (FWHM) of the diamond peaks by using the Scherrer's equation. It is consistent with the TEM observations.

### 3.2 EELS

The EEL spectrum of the outer part of a nanocrystalline diamond particle is shown in Figure 3. It exhibits a peak at 290 eV corresponding to $\sigma^*$ states and a small peak appears at ~285 eV corresponding to $\pi^*$ states. The ELNES above 290 eV is similar to that of diamond [8] and is clearly different from that of graphite or $sp^3$-rich tetrahedral amorphous carbon [9]. The intensity of the $\pi^*$ peak is much lower than that of the $\sigma^*$ peak. Although the $\sigma^*$ peak in general includes contributions from both $sp^2$ and $sp^3$ bonding, the $\sigma^*$ peak of the EEL spectrum in Fig. 3 is considered to be mainly due to $sp^3$ bonding. The use of a narrow energy window positioned on the ELNES signal allows the mapping of the variation in intensity as a function of position within the microstructure. The conventional so-called three-window method [10] was employed to remove the background contribution. Two pre-edge images (272-277 and 277-282 eV), indicated by $\mathbf{a_1}$ and $\mathbf{a_2}$ in Fig. 3, were used to obtain an extrapolated background image. The subtraction of the extrapolated background image from the postedge images (282-287 and 287-292 eV) indicated by **b** and **c** produces the $\pi^*$ and $\sigma^*$ images, respectively, with the background contribution removed.

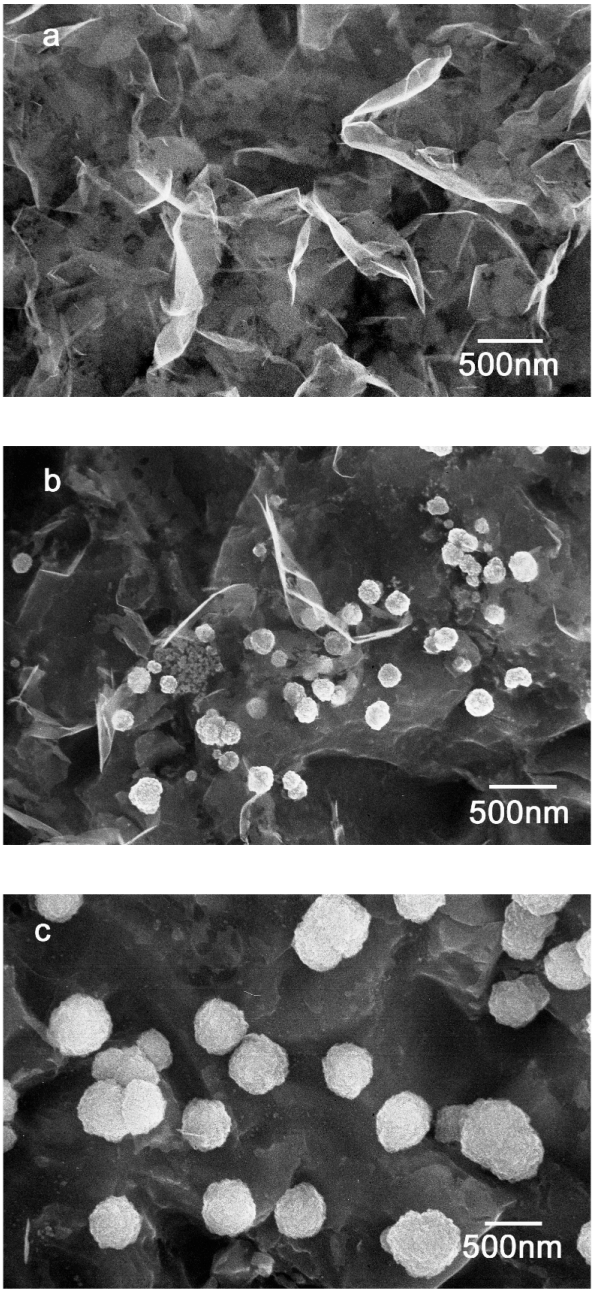


Fig. 2. SEM micrographs of obtained deposits: (a) $[CH_4/CO]$=4.5/0 sccm, (b) $[CH_4/CO]$=4.5/1.0 sccm, and (c) $[CH_4/CO]$=4.5/10 sccm.

The $\pi*$ and $\sigma*$ images of the outer part of a nanocrystalline diamond particle are shown in Figures 4(a) and 4(b), respectively. Since the intensity of the $\pi*$ image was weak compared with that of the $\sigma*$ image, the former was increased by a factor of 5. The $\pi*$ image reveals that the intensity is strong around the subgrains, whereas the $\sigma*$ image shows that the intensity is strong within the subgrains. Although $sp^2$-bonded graphitic layers do not clearly appear because of the limitation at the resolution of the HR-TEM image, these energy-filtered $\pi*$ and $\sigma*$ images imply that $sp^2$ bonding is localized around 20-50 nm subgrains. The $sp^2$ bonding around the subgrains is considered to contribute to the small peak at ~285 eV in the ELNES. The width of the $sp^2$ bonding is estimated to be approximately 1 nm from the $\pi*$ image in Fig. 4(a). Fallon and Brown [11] reported the presence of amorphous carbon at the grain boundaries of CVD diamond films by TEM observation and EELS analysis. The amorphous carbon is shown to contain almost exclusively $sp^2$ bonding and to be nonhydrogenated. It was also demonstrated from the theoretical point of view [12] that $sp^2$ bonding is energetically stable in the grain boundaries of nanocrystalline diamond. It is consequently considered that the $sp^2$ bonding is localized in the grain boundaries of 20-50 nm subgrains.

Figures 5(a) and 5(b) show the low loss region of EEL spectra of a nanocrystalline diamond particle in sample C and a graphite-like platelet in sample A, respectively. The low loss region, extending from 0 to ~50 eV, corresponds to the excitation of electrons in the outermost atomic orbitals and reflects the solid state character of the sample. The low loss region is dominated by collective, resonant oscillations of the valence electrons known as plasmons [10]. In Fig. 5(a), the peak at 33 eV is assigned to the bulk plasmon, $E_B$ of diamond, and the shoulder at 23 eV is attributed to the surface plasmon, $E_S$ of diamond. The $E_S$ is almost equal to the $E_B/\sqrt{2}$, which is consistent with the previous report on diamond [13]. It was also reported [13] that the intensity of surface plasmon peak to that of bulk plasmon peak increases with decreasing crystallite size of nanocrystalline diamond.

On the other hand, the low loss spectrum of a graphite-like platelet as shown in Fig. 5(b) consists of two peaks at 27 eV and 6 eV. The former corresponds to the main plasmon peak of graphite, and the latter to a $\pi$ to $\pi*$ interband transition, which reflects the excitation of valence electrons to low-energy unoccupied electronic states above the Fermi level [10]. The whole spectrum shape is similar to that of graphite reported previously [10].

The author has demonstrated the $sp^2$ bonding distributions in the nanocrystalline diamond particles by the $\pi*$ peak of the high loss region of the EEL spectrum. The mapping of $sp^2$ states reveals that $sp^2$ bondings are localized in the grain boundaries of 20-50 nm subgrains. Thus one can say that the combination of low loss and high loss regions of EEL spectra enables one to perform extensive

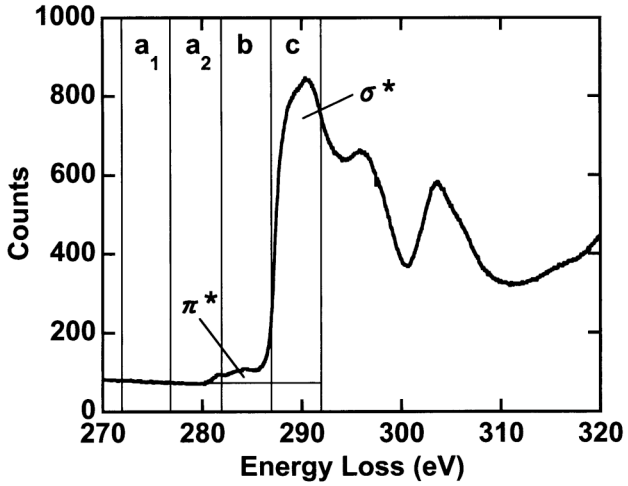


Fig. 3. EEL spectrum of the outer part of a nanocrystalline diamond particle.

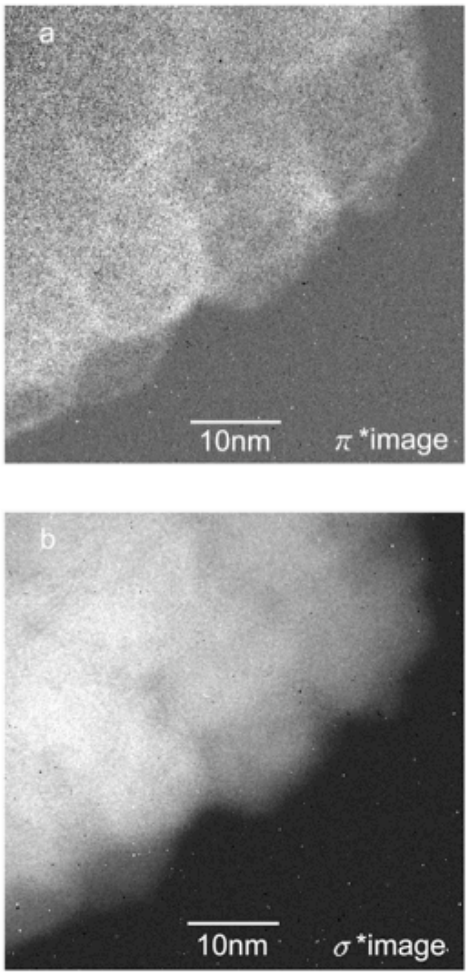


Fig. 4. (a) $\pi*$ image and (b) $\sigma*$ image of the outer part of a nanocrystalline diamond particle.


NSTI-Nanotech 2008, www.nsti.org, ISBN 978-1-4200-8503-7 Vol. 1

characterizations of nanocrystalline diamond and nanostructured carbon.

The nanocrystalline diamond particles of 5 nm diameter as shown in Figure 6 are expected to exhibit an emission in UV region and could be used for an UV-light emitting nanodevice.

## 4 SUMMARY

Nanocrystalline diamond particles of 200-700 nm diameter, two-dimensional platelet-like graphite, and carbon nanotubes were prepared in a 13.56 MHz low pressure inductively coupled $CH_4/CO/H_2$ plasma. The minimum diameter of the particles was found to be 5 nm. The mapping of $sp^2$ bonding by the $\pi^*$ image derived from the EEL spectrum reveals that $sp^2$-bonded carbons are localized in the grain boundaries of 20-50 nm sub-grains of nanocrystalline diamond particles at approximately 1 nm width. The low loss region of EEL spectra exhibits a bulk plasmon peak at 33 eV and a surface plasmon peak at 23 eV. It is concluded in this study that the combination of low loss and high loss regions of EEL spectra enables one to perform extensive characterizations of nanocrystalline diamond and nanostructured carbon.

## REFERENCES


[1] D. M. Gruen, Annu. Rev. Mater. Sci. **29**, 211 (1999).

[2] J. Philip, P. Hess, T. Feygelson, J. E. Butler, S. Chattopadhyay, K. H. Chen, and L. C. Chen, J. Appl. Phys. **93,** 2164 (2003).

[3] J. A. Carlisle, J. Birrell, J. E. Gerbi, O. Auciello, J. M. Gibson, and D. M. Gruen, 8th Inter. Conf. New Diamond Sci. Tech., Melbourne, p. 129, (2002).

[4] G. M. Swain, A. B. Anderson, J. C. Angus, MRS Bull. p.56, (1998).

[5] K. Okada, S. Komatsu, and S. Matsumoto, J. Mater. Res. **14,** 578 (1999).

[6] K. Okada, K. Kimoto, S. Komatsu, and S. Matsumoto, J. Appl. Phys. **93,** 3120 (2003).

[7] K. Okada, H. Kanda, S. Komatsu, and S. Matsumoto, J. Appl. Phys. **88,** 1674 (2000).

[8] R.F. Egerton, M.J. Whelan, J. Elect. Spect. Relat. Phenom. **3,** 232 (1974).

[9] J. Bruley, D.B. Williams, J.J. Cuomo, D.P. Pappas, J. Microscopy **180**, 22 (1995).

[10] R. Brydson, *Electron Energy Loss Spectroscopy*, Springer-Verlag, New York, (2001).

[11] P.J. Fallon, L.M. Brown, Diamond Relat. Mater. **2**, 1004 (1993).

[12] P. Keblinski, D. Wolf, S.R. Phillpot, H. Gleiter, J. Mater. Res. **13**, 2077 (1998).

[13] S. Prawer, K. W. Nugent, D. N. Jamieson, J. O. Orwa, L. A. Bursill, and J. L. Peng, Chem. Phys. Lett. **332,** 93 (2000).


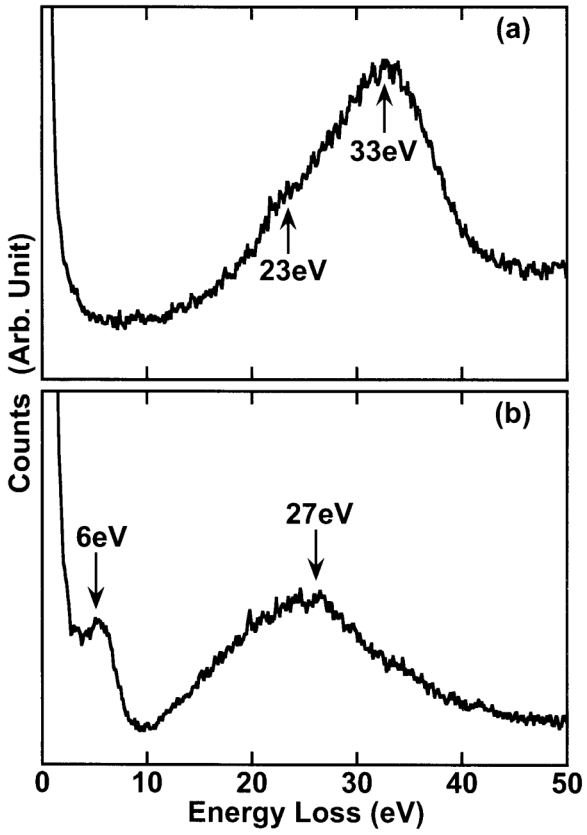


Fig. 5. Low loss spectra of (a) nanocrystalline diamond particle and (b) graphite-like platelet.

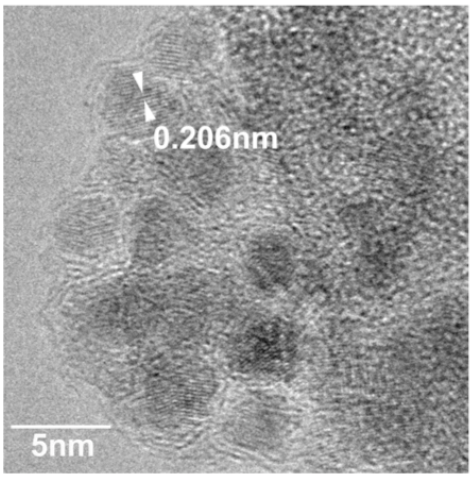


Fig. 6. TEM image of nanocrystalline diamond particles of 5 nm diameter.